View metadata, citation and similar papers at core.ac.uk

brought to you by CORE

provided by Elsevier - Publisher Connector

Available at
www.ElsevierMathematics.com
POWERED BY SCIENCE DIRECT®

Applied Mathematical Modelling 28 (2004) 273–290

APPLIED MATHEMATICAL MODELLING

www.elsevier.com/locate/apm

Simulation of the agglomeration in a spray using Lagrangian particle tracking

Baoyu Guo, David F. Fletcher *, Tim A.G. Langrish

Department of Chemical Engineering, The University of Sydney, Sydney, NSW 2006, Australia

Received 30 September 2002; received in revised form 28 April 2003; accepted 10 June 2003

Abstract

This work aims to explore the possibility of simulating the agglomeration process in a spray using CFD methods. The model system consists of a spray nozzle within a uniform airflow in a square-section chamber. The CFD simulations are performed using a mixed Eulerian–Lagrangian approach. The flow is modelled by solving the usual Eulerian equations, and then representative droplets are tracked using the Lagrangian approach, with conventional gas–particle coupling.

A number of representative particles are introduced at each time step, with each particle representing a group of real particles with the same properties, and are tracked in a transient flow. Due to turbulence, particles are dispersed and may coalesce when they are close. The inter-particle distance is used to calculate the collision probability from kinetic theory, and agglomeration is assumed to occur when the proximity function exceeds a critical value. This method is applied to the simulation of a round spray jet flow, and the results show some interesting insights regarding the role of particle size redistribution and agglomeration. The Sauter mean diameter is found to be the appropriate variable to quantify the agglomeration rate.
© 2003 Elsevier Inc. All rights reserved.

Keywords: Numerical simulation; CFD; Agglomeration; Particles; Lagrangian method; Spray

1. Introduction

A well-controlled particle size distribution is desirable for spray-dried products. Agglomeration takes place inevitably, or is employed for controlling the particle size, in consumer products produced in spray dryers, such as milk powder, coffee and detergents. For these products, a larger

* Corresponding author. Tel.: +61-2-9351-4147; fax: +61-2-9351-2854.
E-mail address: davidf@chem.eng.usyd.edu.au (D.F. Fletcher).

0307-904X/$ - see front matter © 2003 Elsevier Inc. All rights reserved.
doi:10.1016/S0307-904X(03)00133-1

and uniform particle size is preferred for collection, packaging and post-processing applications, although smaller droplets are desirable from the viewpoint of the drying process, due to the enhanced heat and mass transfer rate.

Control of the particle sizes can be achieved by proper arrangement of the atomising nozzles and by controlling the airflow in order to control the agglomeration of the sprayed droplets. However, currently little is understood about the agglomeration process in any quantitative detail for dilute-phase systems, such as spray dryers, with most of the previous work in this area being empirical in nature [7].

Two theoretical approaches are available to solve these two-phase flow problems, namely, the Eulerian and the Lagrangian approaches. The first one solves coupled multi-phase flow equations to treat the multi-size particles as inter-penetrating continua. A review has been given by Gouesbet and Berlemont [14] describing the advantages of each approach. The Eulerian code is usually fast running, but the dispersion tensor introduced in a transport equation for mean number-densities lacks generality. In the Lagrangian approach, the dispersed particles trajectories are followed. In turbulent flows, the Lagrangian approach is well suited to the simulation of complex phenomena, avoiding a significant increase in the number of model constants.

The flowfields in spray dryers are highly transient, three-dimensional and contain recirculating regions, thus significant mixing between dry and wet product is possible. This can be easily handled in a Lagrangian manner, as the history of particles can be tracked, such as residence time, moisture content and particle properties, so this approach is appropriate to take into account complex agglomeration kinetics.

Representative studies of agglomeration include descriptions by Hounslow et al. [17], Hogg [16] and Adams et al. [1]. Publications reviewing particulate media cover a wide range of applications from the agglomeration of droplets in clouds [24] to coagulation in stirred tanks, and flocculation [10,18] and granulation [20]. These approaches all involve the solution of population balances based on unsteady-state mass balances [17]. The most difficult part of modelling agglomeration, in general, is the selection of a collision kernel, due to the complexity and limited knowledge of the forces involved. Bramley et al. [4] and Seyssiecq et al. [25] showed that a size independent kernel resulted in the most suitable description of their experiments on precipitation and crystallisation from liquid solutions.

Discrete particle simulations of the agglomeration process, focussing on the fate of individual particles rather than particle size classes, have also been reported [19]. The structure of the resulting coalesced agglomerate depended on the impact velocity of the interacting particles. As an alternative to the numerical solution of the population balance, a sample of real particles could be tracked using a statistical method (Monte-Carlo). A typical study is that of Rüger et al. [23], in which particle collisions are treated in a purely stochastic way, with a high computational cost due to the need to average the cloud properties over a statistically significant sample of droplets. This approach has been used to simulate liquid spray structures. Gavaises et al. [12] used a spray model, implemented in a CFD code, to study the effect of droplet collisions on spray mixing resulting from the overlapping of liquid cones produced by two parallel nozzles under the influence of a cross-flow.

Particles can be tracked either simultaneously [21] or sequentially one-by-one [26]. In a typical implementation of sequential tracking, a discrete particle may be viewed as surrounded by a cloud of probability associated with this particle. The probability of collision events can be evaluated

assuming that the local particle characteristics are known along a trajectory, such as the particle size distribution function, velocity fluctuation and correlation [26]. Simultaneous tracking of N particles is the most natural approach to account not only for collisions but also for hydrodynamic interactions between particles. The collision probability according to kinetic theory has been used widely [21,23].

Regarding the agglomeration of liquid droplets, Qian and Law [22], have studied binary droplet collisions and their outcomes. Binary droplet collisions exhibit five distinct collision regimes, namely, (I) coalescence with minor deformation, (II) bouncing, (III) coalescence with major deformation, (IV) reflexive separation, and (V) rotational or stretching separation [11]. The collision Weber number, the impact angle and the diameter ratio are often used to characterise the collision process. Generally, it is more difficult for two unequal-size droplets to separate after the collision than for two equal-size droplets. Liquid viscosity also plays a role, since when the interfacial deformation induced by viscous forces between colliding droplets is sufficiently large, the droplets will bounce before the gas is forced out of the gap between them.

The motivation of the present work is to simulate the agglomeration process in spray dryers. In these devices, typical number concentrations are of the order of 10^{11} m^{-3}, which puts the concentrations in the same dilute range as those in crystallisers. In a dilute system, a rate-limiting step is the collision rate, while in a concentrated system, the particles are always assumed to be in contact. In order for particles to agglomerate in spray dryers, particles need to collide and then stick together [16].

The flow pattern of the continuous phase mainly governs the path and velocities of the particles in a dilute system, and therefore affects the agglomeration significantly. The availability of the latest CFD tools has the potential to provide a cost effective means of investigating numerically the mechanisms of agglomeration in order to obtain insight into the agglomeration process, which is an essential first step in controlling it. The current work is a first step in using state-of-the-art computational techniques to gain a fundamental understanding of this phenomenon.

2. Description of the model

2.1. Collision probability

A key submodel in the CFD code is that which determines the collision frequency. The collision calculation is performed for pairs of parcels of particles, without collisions being considered within each parcel. The parcel with the smaller number of particles (N_1) is called a 'collector', and the other parcel with more particles (N_2) is called a 'contributor', where $N_1 \leqslant N_2$. All droplets within the same parcel behave in the same manner, i.e., when one droplet in the collector collides with droplets in the contributor, all the droplets in the collector are likely to collide with droplets in the contributor. Based on kinetic theory, the collision frequency between one droplet associated with a collector and droplets associated with a contributor is proportional to the mean number density, a collision cross-sectional area and the relative velocity [23],

$$v = \frac{N_2}{V} 0.25\pi (d_1 + d_2)^2 u_r, \tag{1}$$

where V is the volume in which both parcels are located. Traditionally most authors use the computational cell (or volume) as a "mixing vessel", thus particles in different cells cannot collide. This could cause serious mesh dependencies if the number of parcels is low in a control cell. The distance between the individual droplets is unknown, since a number of parcels are tracked in the current simulation. Here a physical control volume (CV) is defined by the distance l between the parcels, which can be evaluated as the instantaneous distance at the end of each time step. Eq. (1) becomes,

$$v = \frac{N_2}{b_1 \frac{1}{6}\pi l^3} 0.25\pi (d_1 + d_2)^2 u_r, \tag{2}$$

where b_1 is an empirical constant. This assumes that there is a cloud of real particles surrounding each computational particle, and the interacting volume within the two intersecting spheres has a length scale proportional to the inter-parcel distance. Eq. (2) shows that the average collision frequency is most sensitive to the distance (l). Compared with the traditional computational cell approach, collisions between any particles are possible without restriction by the boundary of the control cell in the current method, with the amount of interaction depending on the collision probability. An advantage of this method is that the simulated collision results tend to be less sensitive to the computational grid, as long as the continuous-phase flow is adequately resolved. It also saves computational time in searching for the parcels that are located within a cell in order to calculate the local number density.

The expected number of collisions between the two parcels of droplets over a short time interval (Δt) is given by

$$\lambda = v\,\Delta t. \tag{3}$$

The probability of m collisions is assumed to follow a Poisson's distribution,

$$p(m) = \frac{1}{m!}\lambda^m e^{-\lambda}. \tag{4}$$

The probability of at least one collision, $p_{coll} = p(m \geqslant 1)$, is complementary to no collisions $p(m = 0)$, giving an expression for the collision probability:

$$p_{coll} = 1 - e^{-\lambda}. \tag{5}$$

All particle pairs are regarded as being in contact and collision outcomes are considered when p_{coll} exceeds a critical value, i.e., $p_{coll} \geqslant 0.5$. Otherwise there is no interaction between the two parcels. This is equivalent to the assumption that coalescence occurs if a "proximity" function, defined as

$$P = \frac{N_2}{l^3}\Delta t (d_1 + d_2)^2 u_r, \tag{6}$$

is sufficiently large. The constant coefficient $1.5/b_1$ is ignored in Eq. (6) for convenience but can be accounted for by a critical proximity, P_c. Thus the criterion for collision events is

$$P \geqslant P_c \equiv -\frac{b_1 \log 0.5}{1.5}. \tag{7}$$

The collision probability, though related to the particle sizes and relative motion, is most sensitive to the inter-parcel distance. The term $(d_1 + d_2)^2 u_r$ is effectively a size-dependent collision kernel, as

used in the population balance equation of the Eulerian approach, since the particle fluctuating velocity and size are usually correlated in turbulent flow.

2.2. Collision outcome

At the end of a time step, the location and velocity components of each particle are obtained. For each pair, a separation vector $\vec{S}$ and a relative velocity vector $\vec{u}_r$ are calculated (Fig. 1). The impact angle is calculated as,

$$\cos\phi = -\frac{\vec{S}\cdot\vec{u}_r}{Su_r}, \quad 0 \leqslant \phi \leqslant \pi. \tag{8}$$

The particle pairs are approaching and are likely to collide only when $\cos\phi \geqslant 0$, otherwise the particle pairs are moving away from each other at that moment, and collision is impossible.

An empirical model based on experimental data was used to describe the outcome of a collision [21]. The discrimination between grazing collision and coalescence is decided by the critical collision angle, which is given by

$$\sin^2\phi_{crit} = \min[1.0, 2.4f(\gamma)/We], \tag{9}$$

where the collision Weber number is defined as

$$We = \frac{\rho u_r^2 d_1}{\sigma}. \tag{10}$$

The function f was fitted by Amsden et al. [2] after analysing the experimental results of Brazier-Smith et al. [5] by

$$f(\gamma) = \gamma^3 - 2.4\gamma^2 + 2.7\gamma, \tag{11}$$

where $\gamma = d_1/d_2$ and $d_1 > d_2$. Note Eq. (9) applies only to water droplets.

If the collision angle ϕ is greater than ϕ_{crit}, then agglomeration is assumed to occur between the colliding parcels. The collector will absorb a part of the colliding contributor, so that each particle in the collector coalesces with one in the contributor on a one-to-one basis to form an agglomerate, leaving the excess particles remaining in the contributor and being tracked further in the

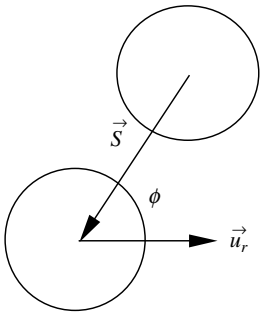

Fig. 1. Relative motion of droplet pairs.

next step. There is normally a transfer of particles from the contributor to the collector, except in the special case $N_1 = N_2$, where a single parcel is formed from the parent parcels. The velocities of the agglomerate are determined by momentum conservation. The particle size in the collector increases and the new particle size is determined according to conservation of volume

$$d^3 = d_1^3 + d_2^3. \tag{12}$$

If the collision angle ϕ is greater than ϕ_{crit}, then the collision is a grazing collision, so the droplets maintain their size but undergo velocity changes. The velocity of a droplet after a grazing collision is

$$\vec{u}_1' = \frac{\vec{u}_1 m_1 + \vec{u}_2 m_2 + m_2(\vec{u}_1 - \vec{u}_2)[(\sin\phi - \sin\phi_{\text{crit}})/(1 - \sin\phi_{\text{crit}})]}{m_1 + m_2}. \tag{13}$$

2.3. The simulation procedure

The airflow field needs to be solved first, but gas–particle coupling is accounted for iteratively after the particle trajectories are calculated. The three-dimensional Reynolds-averaged Navier–Stokes equations, together with the k–ε turbulence model, are discretised on a structured mesh, and the flow variables, such as velocities and turbulence intensity, are solved to obtain their values at a number of grid nodes (Eulerian approach). The simulations use CFX4.4, a finite volume based code [6]. The mesh is rectangular and non-uniform, with the grid density being gradually refined as the nozzle is approached in order to resolve the flow variation properly in the region of high particle concentration.

Due to the dispersed nature of the particle phase, a time-dependent simulation has been carried out, although a steady-state flow is expected for a single-phase flow in this simple geometry. However, the transient simulation approach can be easily applied to oscillating flows or unstable flows, such as swirling flows behind a sudden expansion [15]. This approach also facilitates constant injection of particles with time and allows for the interaction of particles throughout time. Thus both intermittent and continuous processes can be modelled.

Newton's law of motion is solved for the particles, giving the velocities and locations of particles as a function of time. The effect of turbulence is included within the particle transport model using the method of Gosman and Ioannides [13]. The continuum velocity in the momentum equations is taken to be the mean velocity plus a contribution due to turbulence.

All particles, including those that are newly injected and those that have already been injected in previous time steps, are tracked within the current time interval unless they have left the simulated region. The drag force is added to the fluid momentum equation as a source. A number of iterations are carried out until the two-way coupling between the particles and the fluid converges. Alternatively, a one-way transient particle tracking calculation starts from steady simulation result, in which two-way coupling has been carried out without agglomeration. This saves CPU time without affecting the main results, such as d_{32} at the exit, for the cases studied here where there is only limited agglomeration.

An integral time scale can be calculated as the residence time based on the mean velocity for the continuous phase (gas flow). The time step used is two orders of magnitude smaller. At the end of

each time step, the state of each particle is identified, i.e., whether it is waiting for the next time step or it has left the domain. The diameters, velocities and physical locations for the waiting particles are retrieved for the implementation of the agglomeration model. The particle pairs that fall within a pre-set proximity are identified, which may involve particles that started at different times. As a model parameter, the critical value of the proximity for collision, P_c, depends on the model constant, b_1, which needs to be evaluated by fitting experimental data when available. In the current simulation, $b_1 = 5$ was arbitrarily chosen for the base case, which corresponds to the assumption that the interacting volume is five times that of the sphere with a diameter equal to the inter-parcel distance.

Only binary interaction is considered in each time step, but multiple particle agglomeration is possible as time advances. When more than one pair of particles falls in the pre-set criteria, the closest pair coalesces with priority. Care has been taken to avoid multiple counting. The initial velocities of the agglomerate are determined based on momentum conservation. The new particle location is the mass-weighted average of the co-ordinates of the parent particles. The parent particles are removed from the calculation, whereas the newly created agglomerates are included together with the newly injected ones from the nozzle. Therefore, during each time step interval, three categories of particles are being tracked, i.e., the existing particles in the domain, the newly created agglomerates and the newly injected particles from the nozzle.

As time advances in the simulation, quasi-steady state conditions are established, i.e., the total number of particles that leave the domain, the particles being tracked and the agglomerates created become nearly constant. About 10,000 particles remained in the domain under quasi-steady state conditions. It takes about 0.05 s of simulation time before the quasi-steady state is achieved, which is of the same order as the integral time scale of the airflow. The initial period of simulation time has been disregarded prior to the analysis step, so that the data are sampled in the quasi-steady state conditions and thus are reproducible. The quasi-steady state is further confirmed by the fact the total volume flux for the particle phase is conserved along the stream, since mass transfer to the gas phase is not considered.

2.4. The boundary conditions

The case study is a round water spray in a turbulent jet flow. The jet is generated from a tubular nozzle with a diameter of $D = 9.8$ mm and a mean gas velocity of 50 m/s. The Reynolds number at the nozzle exit is about 37,000. The mean turbulent intensity is set as 3.7% and the dissipation length scale is set as the tube diameter. These values are close to a fully developed pipe flow. In order to simplify the gas flow pattern, the nozzle is placed in a 3 m/s co-flowing air stream with 2% turbulence intensity, which makes the flow parabolic. The initial mean particle velocity is 50 m/s without any radial component. The simulation domain starts from the nozzle exit plane to $30D$ downstream, with a square cross-section of 0.2×0.2 m.

The initial particle injection locations are constructed in such a way that the particle number density is highest at the centreline and decreases linearly with radius. A number of representative particles (parcels) with a single size or a group of sizes, are injected at each time step, which carry a total flowrate of 1.0 kg/h. The number of real particles in each parcel is tuned in order to meet a prescribed size distribution function, e.g., a lognormal distribution function. The average mass loading at the jet inlet is 5%.

3. Results

During the transient simulation, particle information for each parcel, including the number of particles, sizes, velocities and locations, are recorded at the end of each time step, so that instantaneous properties over a period of time are obtained. The cone-shaped space taken by the spray is divided into a number of control volumes in a post-processor, where the stochastic data are averaged. In each control volume, the total number flux that passes through the cross-section of the CV is calculated based on the particle velocities. Except for the number density, most mean properties, such as Sauter diameter d_{32}, are flux based, since the total volume flux is a conserved quantity along the stream for a steady flow.

Although the simulations are transient and three-dimensional, the results are processed by time averaging in an axisymmetric co-ordinate system. Spatial variation of particle properties is described by means of integral values (integrated/averaged over a cross-section/exit) and local values (along the centreline and radial profiles).

3.1. No agglomeration

The understanding of the flow behaviour is fundamental before investigating the effect of agglomeration. A range of 25 particle size classes are injected with the agglomeration model switched off. Figs. 2 and 3 show the radial profiles of mean axial velocity for the gas flow and particle flow, respectively. By comparing the mean velocity profiles for the two phases it is evident that the gas jet flow spreads faster than that of the particle phase. The velocity of the gas phase decays more quickly than that of the particle phase, although they are equal initially for both phases. Thus a slip velocity is created due to the inertia of the particles, which is clearly visible before 20D from the nozzle. Further downstream, this slip velocity becomes negligible.

The instantaneous velocities reflect, to a large extent, the response of particles to the continuous flow. Fig. 4 shows the particle velocities for different sizes at a centreline point 20D downstream. On average, the axial velocity increases with the particle sizes, because the large particles tend to retain their initial velocities due to inertia, whereas the smaller particles follow the mean gas flow. The velocity deviations from the mean values are also related to the particle sizes, and larger

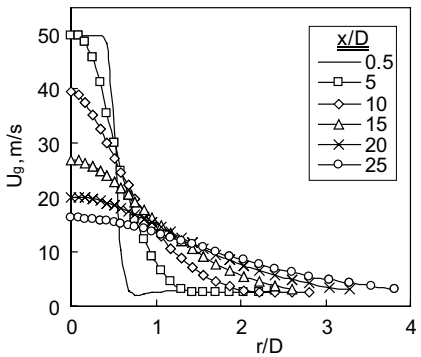

Fig. 2. Radial profile of the axial velocity at different axial locations for the gas phase.

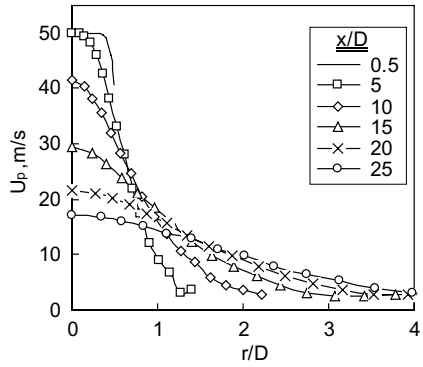

Fig. 3. Radial profile of the axial velocity at different axial locations for the particle phase.

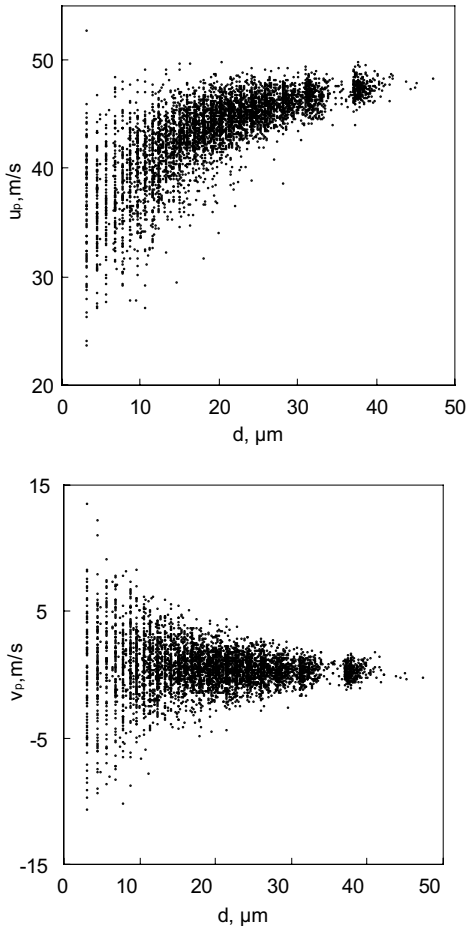

Fig. 4. Correlation of axial and radial velocity with particle size at the centreline 20*D* from inlet.

particles have weaker velocity fluctuations than the smaller ones. This result agrees with the experimentally measured behaviour under similar flow conditions [8,9]. Also this is not inconsistent with the concept of equal partition of kinetic energy [3] used in a coalescence kernel to describe fluidised bed granulation, i.e., the kinetic energy is distributed evenly amongst the particles independent of their size. However, larger particles in the current simulation possess a larger kinetic energy based on the particle velocity fluctuations (average velocity deviations from their mean value). This is due, to some extent, to the fact that the turbulence in the jet flow is strongly inhomogeneous and decays with the distance from the nozzle. The large particles are able to "memorise" their previous conditions along their trajectory, leading to stronger velocity variations. Due to strong particle velocity fluctuations, the fine particles disperse more quickly from the centreline than the coarse particles in the radial direction, resulting in a radial redistribution of particle sizes.

Fig. 5 shows the variation of d_{32} for both the integral value over the stream and the local value at the centreline. The integral mean particle sizes remain constant along the stream, indicating that the particle flow has reached a steady-state balance. The local mean particle size at the centreline is generally higher than the average due to the radial dispersion of fine particles, which is clearly shown by the radial profiles of the mean particle sizes, as shown in Fig. 6.

However, the mean particle size at the centreline increases initially before 15D and then decreases slightly further downstream, which is partly due to a slip velocity between different sizes in the axial direction. Although all the particles are injected with the same initial velocity, fine particles slow down quickly in the streamwise direction due to smaller particle relaxation times, thus a velocity difference is created among particles of different sizes. Fine particles, once injected, also spread quickly in the radial direction following the gas flow, giving a large d_{32} at the centreline. Meanwhile, fine particles accumulate in terms of number density relative to large particles, due to the lower velocity of small droplets than that of large ones. Consequently the particle size distribution differs between particles that reside in a particular volume and those that pass through a cross-section at a particular location, with d_{32} being smaller for the former than for the latter case (as shown in Fig. 7). This velocity difference becomes insignificant as the large

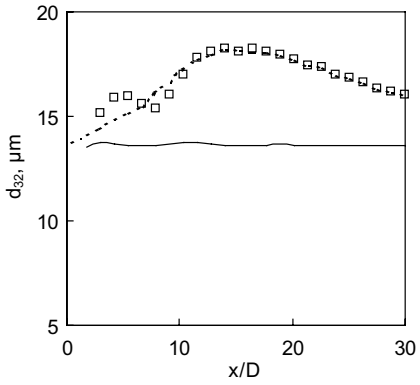

Fig. 5. Streamwise variation of the mean size d_{32} for the case of no agglomeration (solid line: integrated over the cross-section; dash line: trend-line along the centre axis; square symbol: at the centreline obtained by volume averaging).

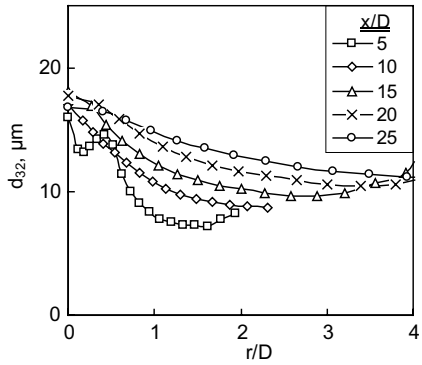

Fig. 6. Radial profile of mean particle size d_{32} at different axial locations without agglomeration.

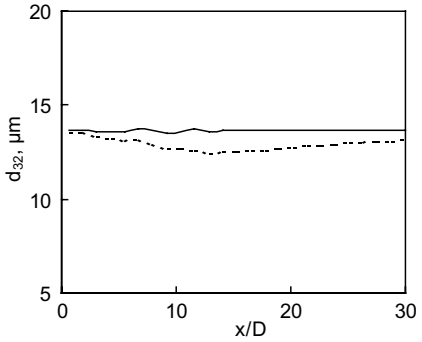

Fig. 7. Streamwise variation of integral mean size d_{32} for the case of no agglomeration showing the effect of fine particle accumulation (solid line: flux-based; dash line: volume based).

particles slow down further downstream, which leads to the accumulation and decrease in flux of large particles, reducing the mean size slightly. In this case, the value of d_{32} becomes equal for the resident and flowing particles.

3.2. Agglomeration with a mono-size inlet stream

Fig. 8 shows the particle size distributions resulting from a simulation with an initially uniform size of 10 μm. Although particles of a uniform particle size were injected, a finite number of particle sizes have been obtained in the simulation due to coalescence between the original particles, between the original particles and agglomerates, and between agglomerates. Due to the single initial particle size, coalescence gives a discrete series of particles sizes, with the volume of any agglomerate being an integer multiple of the original particle volume. In other words, the intervals of these discrete sizes, in terms of volume, are most likely to be equal to the minimum particle volume, corresponding to a decreasing interval in diameter as the diameter increases. The smallest size is always equal to the initial size, since droplet breakup is not considered.

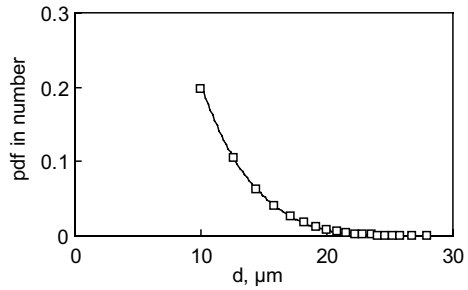

Fig. 8. Particle size distribution at the exit for the case of mono-size particle injection.

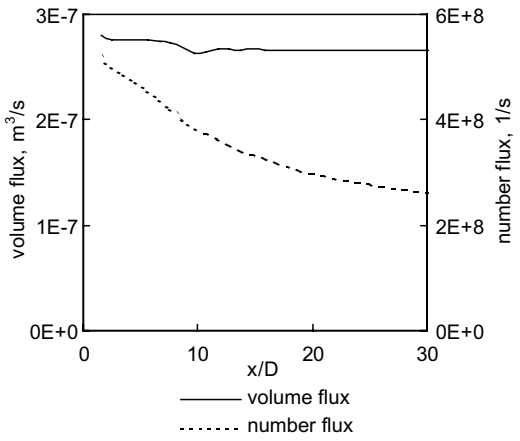

Fig. 9. Streamwise variation of total volume flux and number flux integrated over a cross-section for the case of a single initial size.

The integral number flux decreases with distance from the inlet due to the coalescence of particles, although the total volume/mass flowrate remains unchanged within 2% (Fig. 9). The integral mean size d_{32} increases steadily with x/D, indicating that agglomeration is not restricted to the near-nozzle region (Fig. 10). In the region close to the nozzle ($x/D < 10$), the large mean particle size occurs at the centreline and decreases with r/D. In this region, the agglomeration rate is controlled by the number density, which is highest at the centreline. For this reason, the gradient of d_{32} along the centreline is higher initially but becomes smaller downstream. Then, as more particle sizes are created by the agglomeration process, the particle size redistribution in space becomes significant because particles of different sizes respond differently to the gas flow. The mean particle size is still relatively large at the centreline (Fig. 11). This is because the finer particles are more likely to follow the gas flow, dispersing more in the radial direction and leaving the larger particles behind at the centre. However, the large particles, once they have gained radial momentum from turbulence, travel further than the fine particles do. This explains why d_{32} increases at the spray edge, although the number of particles in this region is very low.

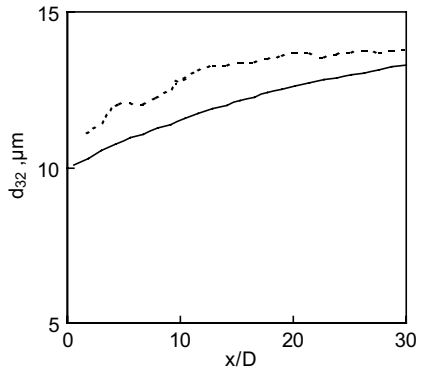

Fig. 10. Streamwise variation of the mean size d_{32} for the case of a single initial size (solid line: integrated over the cross-section; dash line: value at the centreline).

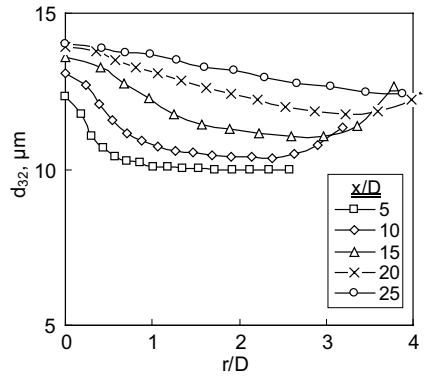

Fig. 11. Radial profile of mean particle size d_{32} at different axial locations for the case of a single initial size.

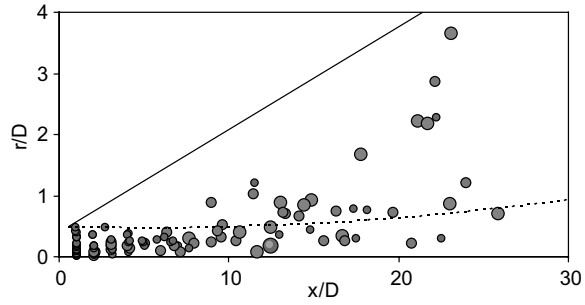

Fig. 12. A snapshot of the distribution of agglomerates for the case of a single initial size $d_0 = 10$ μm (bubble diameter scaled to particle diameter in the range 10–21.5 μm; solid line: spray edge; dash line: peak of turbulent kinetic energy for gas flow).

Fig. 12 highlights the size and spatial distribution of the agglomerates that occur at a specific instant. Agglomeration initially occurs mostly near the centreline due to the high number density. Downstream of the inlet, the number density increases in the shear layer, due to the radial dispersion of particles from the centreline towards the spray edge. Meanwhile, the strong turbulence in the shear layer enhances the mixing of particles, leading to more collisions. Therefore the number of collision events in the shear layer is greater than that in the central region downstream, although the number density is always highest at the centreline. As the shear layer develops, agglomeration occurs over a larger region. In the outer section of the spray, collision rarely occurs because of the low number density and velocity.

3.3. Agglomeration with multiple sizes

The particle initial conditions are identical to those in the case of no agglomeration, except the agglomeration model is used. The particle number density is the most critical parameter for the collision probability. The number density peaks at the centreline and decreases radially towards the spray edge. Generally, the centreline value decreases logarithmically with distance x/D (Fig. 13), and the radial profiles becomes flatter downstream. Agglomeration has apparently reduced the number density in the central region, although both cases show a similar trend. However, it is noted from Fig. 13 that, common to both cases, the centreline number density shows a local recovery at about $x/D = 7$, which corresponds to the limit of the potential core in the jet flow. This phenomenon is not caused by agglomeration, but is the consequence of particle accumulation due to an abrupt decrease in the axial gas velocity, which also accounts for the upstream oscillation of d_{32} along the centreline.

Fig. 14 shows a comparison of the particle size distribution between the inlet and the exit. The curve becomes broader after agglomeration. In this case, the number fraction above 10 μm has increased at the expense of small droplets below 10 μm.

Fig. 15 shows the variation of d_{32} for both the integral value over the stream and the local value at the centreline. The integral mean size d_{32} (solid line) increases monotonically with distance from the inlet, which is consistent with the case of a single initial size. The dashed line represents the

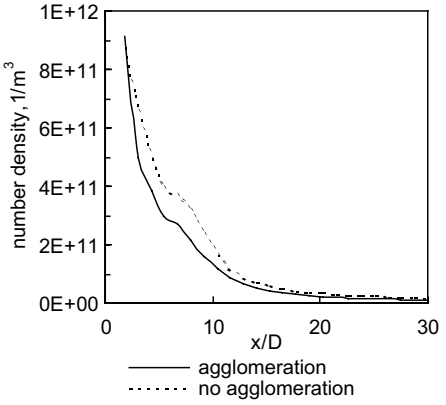

Fig. 13. Variation of particle number density along the centreline for a case with multiple initial sizes.

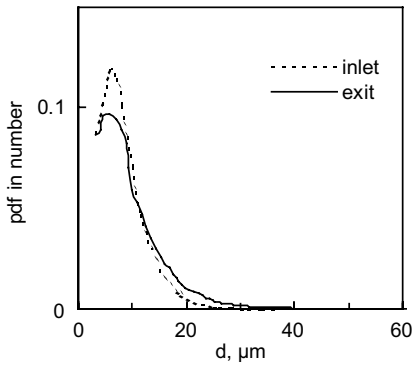

Fig. 14. The effect of agglomeration on the particle size distribution for a case with multiple initial sizes.

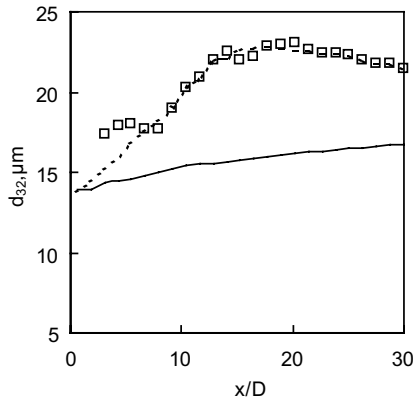

Fig. 15. Variation of the mean size d_{32} with axial distance for the case of multiple sizes (solid line: integrated over the cross-section; dash line: trend-line along the centre axis; square symbol: at the centreline obtained by volume averaging).

centreline mean size. The initial increase of d_{32} is a combined effect of agglomeration and spatial redistribution of particle sizes (as explained in the case of no agglomeration). Near the nozzle, a higher degree of agglomeration is expected at the centreline due to the high number density. The number density decreases with x/D due to the dispersion of particles and agglomeration, therefore the frequency of collision events decreases at the centreline. However, the chance of coalescence becomes higher in the shear layer than at the centre due to the high turbulent velocity fluctuations in the shear layer. Consequently, d_{32} becomes relatively stable along the centreline, although agglomeration is occurring away from the centreline.

By comparing Fig. 16 with Fig. 6, it can be seen that agglomeration has not significantly affected the appearance of the radial profiles for d_{32}, except that the mean size has increased in the central region of the spray. The reason for the similarity is that the small proportion of agglomerates (of the order of 1% in the current simulation) has not significantly changed the initial particle size distribution, which is important for the particle flow redistribution.

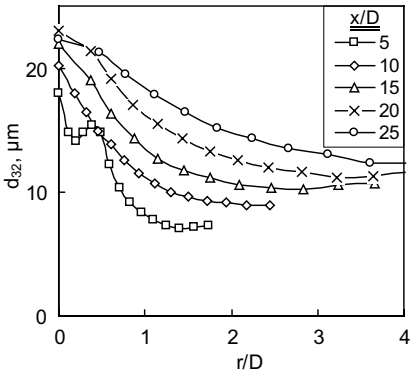

Fig. 16. Radial profile of mean particle size d_{32} at different axial locations for the case of multiple sizes.

3.4. Parametric study of model parameters

It is important to establish the influence of numerical and model assumptions on the agglomeration process. The sensitivity has been assessed by comparison of the mean particle size d_{32} at the exit for a number of parameters, including numerical (the total number of computational particles and the size of the time step), the model constant, b_1 and physical parameters (the initial particle size). In the base case, about 200 representative particles of 10 μm are injected to represent the jet in a time step of $\Delta t = 0.5$ ms. d_{32} is basically insensitive (within 2%) to the number of particles used and the time step when doubling and halving their values.

Whether two particles collide is determined by the collision probability that is related to the proximity function and a model constant b_1 which defines the interacting volume, with a larger value allowing less agglomeration. The mean size difference between the exit and the inlet (a measure of agglomeration rate) changed by 40% when doubling or halving the value for b_1 for the base case of $d_0 = 10$ μm.

Given the total particle mass flowrate, the effect of the initial particle sizes has been examined for the range of 3–30 μm. The mean particle size d_{32} at the exit increases with the initial size, and is

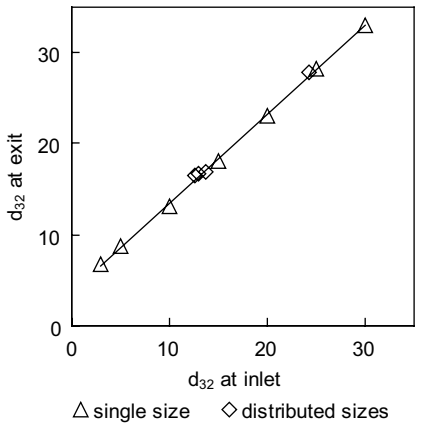

Fig. 17. The effect of initial droplet size on the mean particle size at the exit.

always greater than the initial particle size at the inlet, since only agglomeration is considered. However, this difference become smaller as the initial size increases, because the number density decreases significantly as the particle size increases, which effectively reduces the collision frequency. A smaller initial droplet size gives a broader distribution than for a larger initial size. For the case of a multiple size spray, the distribution of particle sizes becomes broader at the exit. However, d_{32} is not sensitive to the initial particle size distribution, regardless of whether it is a mono-disperse size or a distributed range of sizes (Fig. 17). d_{32} is, by definition, the ratio of mean volume to the mean surface area. The particle number density is inversely proportional to the mean particle volume, for a given volume flowrate. The proximity function is roughly related to d_{32}, meaning that d_{32} is appropriate to describe the agglomeration rate.

4. Conclusions

Numerical simulation has been carried out to model the agglomeration of particles in a dilute system. The particles are tracked using the simultaneous Lagrangian approach, which is incorporated in a transient flow solver in a CFD code, CFX4.4. The current simulations ignore mass and heat transfer between the two phases for simplicity. Due to the inclusion of turbulent dispersion, particles tend to disperse and to collide with each other in a stochastic way. The collision probability was calculated based on kinetic theory, and the number density is approximated by the distance of the representative particles. In a deterministic way, collision occurs when two particles are close, determined via a proximity function, leading to growth in the mean size along the stream and a particle size distribution at the outlet. The collision may result in agglomeration, which is determined by the calculated collision angle.

The method was applied to the simulation of a jet spray flow. The change in Sauter mean diameter was found to be the most appropriate means to quantify the amount of agglomeration. The effect of agglomeration on the particle size redistribution was discussed. Based on this fundamental work, future work will validate the current procedure. In the case of the jet spray flow, the gradient of the integral mean size, d_{32}, along the stream is needed in order to determine the model constant b_1. The variation of the mean size along the centreline can be affected both by particle size redistribution and by agglomeration, which should be examined separately. In order to achieve this we are currently collecting data for a variety of spray jet configurations using various experimental techniques, including PDPA and a laser diffraction size analyser. The validation of the current model using these data will form the subject of a future paper.

Acknowledgement

Funding of this work via an Australian Research Council grant is gratefully acknowledged.

References

[1] M.J. Adams, M.A. Mullier, J.P.K. Seville, Agglomeration, in: B.J. Briscoe, M.J. Adams (Eds.), Tribology in Particulate Technology, Adam Hilger, Bristol, 1987, pp. 375–389.

[2] A.A. Amsden, P.J. O'Rourke, T.D. Butler, KIVA-II: A computer program for chemically reactive flows with sprays, Los Alamos Natl. Lab. Rep LA-11560-MS, Los Alamos, NM, 1989.
[3] C.A. Biggs, R. Boerefijn, M. Buscan, A.D. Salmon, M.J. Hounslow, Fluidised bed granulation: modelling the growth and breakage kinetics using population balances, in: Proceedings of the 4th World Congress on Particle Technology, Sydney, 21–25 July, 2002, Paper no. 226.
[4] A.S. Bramley, M.J. Hounslow, R.L. Ryall, Aggregation during precipitation from solution: a method for extracting rates from experimental data, Journal Colloid Interface Sci. 183 (1) (1996) 155–165.
[5] P.R. Brazier-Smith, S.G. Jennings, J. Latham, The interaction of falling water drops: Coalescence, Proc. R. Soc. Lond. A 326 (1972) 393–406.
[6] CFX, CFX-4.4: Solver Manual, CFX International, AEA Technology, Online documentation.
[7] J.M. Chawla, Effect of the droplet agglomeration on the design of spray dryer towers, Dry. Technol. 12 (6) (1994) 1357–1365.
[8] Y.-C. Chen, Personal communication, 2002.
[9] Y.-C. Chen, S.H. Starter, A.R. Masri, Combined PDA/LIF measurements in simple, evaporating turbulent spray jets, in: Proceedings of the 14th Australasian Fluid Mechanics Conference, Adelaide, Australia, 10–14 December, 2001.
[10] G.B.J. de Boer, C. de Weerd, D. Thoenes, Coagulation in turbulent flows. Part 2, Chem. Eng. Res. Des. 67 (1989) 308–315.
[11] J.P. Estrade, H. Carentz, G. Lavergne, Y. Biscos, Experimental investigation of dynamic binary collision of ethanol droplets—a model for droplet coalescence and bouncing, Int. J. Heat Fluid Flow 20 (5) (1999) 486–491.
[12] M. Gavaises, A. Theodorakakos, G. Bergeles, G. Brenn, Evaluation of the effect of droplet collisions on spray mixing, Proc. Inst. Mech. Eng. C 210 (1996) 465–475.
[13] A.D. Gosman, E. Ioannides, Aspects of computer simulation of liquid-fuelled combustors, J. Energy 7 (6) (1983) 482–490.
[14] G. Gouesbet, A. Berlemont, Eulerian and Lagrangian approaches for predicting the behaviour of discrete particles in turbulent flows, Prog. Energy Combust. Sci. 25 (1999) 133–159.
[15] B. Guo, T.A.G. Langrish, D.F. Fletcher, Simulation of turbulent swirl flow in an axisymmetric sudden expansion, AIAA J. 39 (1) (2001) 96–102.
[16] R. Hogg, Agglomeration model for process design and control, Powder Technol. 69 (1992) 69–76.
[17] M.J. Hounslow, R.L. Ryall, V.R. Marshall, A discretized population balance for nucleation, growth and aggregation, AIChE J. 34 (11) (1988) 1821–1832.
[18] P.T.L. Koh, J.R.G. Andrews, P.H.T. Uhlherr, Modelling shear-flocculation by population balances, Chem. Eng. Sci. 42 (2) (1987) 353–362.
[19] G. Lian, C. Thornton, M.J. Adams, Discrete particle simulation of agglomerate impact coalescence, Chem. Eng. Sci. 53 (19) (1998) 3381–3391.
[20] J.D. Litster, R. Sarwono, Fluidised bed granulation: studies of agglomerate formulation, Powder Technol. 88 (2) (1996) 165–172.
[21] P.J. O'Rourke, Collective Drop Effects on Vaporising Liquid Sprays, Ph.D. Thesis, Los Alamos Natl. Lab., Los Alamos, NM, 1981.
[22] J. Qian, C.K. Law, Regimes of coalescence and separation in droplet collision, J. Fluid Mech. 331 (1997) 59–80.
[23] M. Rüger, S. Hohmann, M. Sommerfeld, G. Kohnen, Euler/Lagrange calculations of turbulent sprays: the effect of droplet collisions and coalescence, At. Sprays 10 (2000) 47–81.
[24] P.G. Saffman, J.S. Turner, On collision of drops in turbulent clouds, J. Fluid Mech. 1 (1956) 16–30.
[25] I. Seyssiecq, S. Veesler, D. Mangin, J.P. Klein, R. Boistelle, Modelling gibbsite agglomeration in a constant supersaturation crystallizer, Chem. Eng. Sci. 55 (2000) 5565–5578.
[26] M. Sommerfeld, Validation of a stochastic Lagrangian modelling approach for inter-particle collision in homogeneous isotropic turbulence, Int. J. Multiph. Flow 27 (2001) 1829–1858.